RESEARCH   **Open Access**

Oral delivery of Sunitinib malate using carboxymethyl cellulose/poly(acrylic acid-itaconic acid)/Cloisite 30B nanocomposite hydrogel as a pH-responsive carrier

Zahra Sayyar[1*], Parisa Mohammadzadeh Pakdel[2] and Seyed Jamaleddin Peighambardoust[2*]

Abstract

This work aimed to fabricate a Cloisite 30B-incorporated carboxymethyl cellulose graft copolymer of acrylic acid and itaconic acid hydrogel (Hyd) via a free radical polymerization method for controlled release of Sunitinib malate anticancer drug. The synthesized samples were characterized by FTIR, XRD, TEM, and SEM-dot mapping analyses. The encapsulation efficiency of Hyd and Hyd/Cloisite 30B (6 wt%) was 81 and 93%, respectively, showing the effectiveness of Cloisite 30B in drug loading. An in vitro drug release study showed that drug release from all samples in a buffer solution with pH 7.4 was higher than in a buffer solution with pH 5.5. During 240 min, the cumulative drug release from Hyd/Cloisite 30B (94.97% at pH 7.4) is lower than Hyd (53.71% at pH 7.4). Also, drug-loaded Hyd/Cloisite 30B (6 wt%) demonstrated better antibacterial activity towards *S. Aureus* bacteria and *E. Coli*. High anticancer activity of Hyd/Cloisite 30B against MCF-7 human breast cancer cells was shown by the MTT assay, with a MCF-7 cell viability of $23.82 \pm 1.23\%$ after 72-hour incubation. Our results suggest that Hyd/Cloisite 30B could be used as a pH-controlled carrier to deliver anticancer Sunitinib malate.

Keywords Sunitinib malate, Nanocomposite hydrogel, Carboxymethyl cellulose, Cancer therapy

Introduction

Drug delivery systems (DDS) have recently gained a special place in clinical applications due to controlled drug release, good biocompatibility, and excellent mechanical strength. Bio-based systems are developed to enhance permeability and drug bioavailability, reduce side effects, and prolong release time. Hydrogels have a three-dimensional structure capable of absorbing large volumes of water or biological fluids due to their hydrophilic structure [1]. Due to the presence of ionizable functional groups such as $-COOH$, $-SO_3H$, and $-CONH_2$, they can be used in intelligent DDS, especially in the delivery of anticancer drugs due to the acidic nature of cancer cells (pH 6.5-7) [2]. Many researchers have studied the application of pH-responsive hydrogels to deliver anticancer drugs such as doxorubicin, methotrexate, and Sunitinib malate. Carboxymethyl cellulose (CMC), as an essential class of cellulose derivate, is an anionic, non-toxic, low-cost, renewable, biocompatible, and biodegradable biopolymer with a wide application in food packaging, wastewater treatment, tissue engineering, wound

*Correspondence:
Zahra Sayyar
z_sayyar@ubonab.ac.ir
Seyed Jamaleddin Peighambardoust
j.peighambardoust@tabrizu.ac.ir
[1] Department of Chemical Engineering, University of Bonab,
Bonab 55513-95133, Iran
[2] Faculty of Chemical and Petroleum Engineering, University of Tabriz,
Tabriz 5166616471, Iran

dressing, and drug delivery. Due to its hydrophilic nature, it can be used to synthesize hydrogel systems [3]. Besides these excellent properties, it suffers from low mechanical strength and low drug encapsulation that can be promoted by grafting ionizable monomers such as acrylic acid (AA), methacrylic acid (MMA), itaconic acid (IA), and their copolymers [4]. As reported in studies, grafting these monomers can induce sensibilities to various body stimuli such as pH, ionic strength, and temperature [5]. AA monomer comprises a vinyl group ($CH_2=CH-$) and a carboxylic acid group ($-COOH$) attached to a carbon atom. The vinyl group allows AA to undergo polymerization reactions to form long chains of polymers. AA monomers can undergo copolymerization reactions with other monomers, such as IA or MAA, to produce copolymers with specific properties. Itaconic acid, with the chemical formula of $C_5H_6O_4$, is classified as a dicarboxylic acid due to its two carboxylic acid functional groups ($-COOH$) attached to a carbon-carbon double bond [6–9]. IA is produced through fermentation by certain microorganisms, including the filamentous fungus Aspergillus terreus [10–12]. It is a versatile compound with diverse industrial applications, especially bio-based products.

Another strategy to enhance mechanical strength and drug encapsulation is the incorporation of various mineral nanoparticles such as clay [13], graphene oxide [14], and halloysite [15]. Cloisite 30B is a synthetic organoclay derived from natural two-dimensional clay minerals. It has a layered structure and a negative surface charge due to the presence of methyl, tallow, bis-2 hydroxyethyl, and quaternary ammonium components. Incorporating Cloisite 30B nanosheets into hydrogel structures promotes their mechanical and thermal characteristics while fostering their antibacterial and drug-loading/releasing capabilities [16, 17]. Madusanka et al. [18] prepared CMC/Cloisite 30B nanocomposite as a novel drug delivery system for curcumin. Monalisha Boruah et al. [19] synthesize CMC-g-P(AA)/OMMT nanocomposite hydrogel to deliver vitamin B12. The results showed that in vitro blood compatibility was enhanced by incorporating OMMT. Mohammadi et al. [20] studied the delivery of doxorubicin hydrochloride (DOX) and 5-fluorouracil (5-FU) by CMC-g-P(AA)/starch-modified Fe_3O_4 nanocomposite. The outcomes showed that the release amount at pH 7.4 was higher than 1.2. Sood et al. [21] synthesized CMC-g-P(LA-co-IA) nanocomposite hydrogel to deliver amoxicillin. Based on their results, synthesized hydrogel showed higher antibacterial activity against gram-positive *S. Aureus* than gram-negative *E.Coli*.

Sunitinib malate is a medication that is mainly used to treat some types of cancer [22]. It is a member of the tyrosine kinase inhibitor (TKI) medication class, which

acts by preventing aberrant proteins from acting that encourage the proliferation of cancer cells [23]. It is commonly prescribed for the treatment of advanced kidney cancer and gastrointestinal stromal tumors that have metastasized to other areas of the body or that are not surgically removable [24, 25].

This study aims to design and synthesize an efficient, non-toxic, and pH-responsive carrier for delivering Sunitinib malate as an anticancer drug model. To our knowledge, no research has been conducted on delivering Sunitinib malate using Hyd and Hyd/Cloisite 30B. The structural characteristics of Hyd and Hyd/Cloisite 30B were assessed using FTIR, XRD, TEM, and SEM-dot mapping techniques. The impact of Cloisite 30B content and pH of media on swelling and drug release behavior of all samples was investigated in detail. The effect of Cloisite 30B content on the antibacterial activity of samples was studied using gram-negative *E. Coli* and gram-positive *S. Aureus* bacteria. Also, the MTT test was applied to study the cytotoxicity and biocompatibility of the drug@Hyd/Cloisite 30B.

Materials and methods
Materials
Acrylic acid (AA, 99.0%), itaconic acid (IA, 99.0%), and N, N-methylene bisacrylamide (MBA, 99.5%) were supplied from Merck (Germany). Potassium persulfate (KPS, 98.0%) was purchased from Samchun Co (Korea). Carboxymethyl cellulose (CMC, degree of substitution 0.9, and average molecular weight 250,000), sodium hydroxide (NaOH), and Sunitinib malate were purchased from Sigma-Aldrich (USA). Cloisite 30B nano-sheets were bought from Neutrino Co. The MCF-7 cell line (human breast cancer cells; ATCC HTB-22) and L929 cell line (mouse fibroblast cells; ATCC CCL-1) were purchased from the Iranian Genetic Resources Center in Tehran, Iran. *Escherichia Coli* (ATCC 25922) and *Staphylococcus Aureus* (ATCC 25923) were bought from the Pasteur Institute of Iran (PII, Tehran, Iran).

Preparation of Hyd/Cloisite 30B
A free radical polymerization method was applied to synthesize Hyd/Cloisite 30B. A viscous CMC solution (1% w/v in 10 mL distilled water) was prepared under an N_2 atmosphere in a four-necked flask equipped with a stirrer, a thermometer, a nitrogen line, and a reflux condenser. After reaching the temperature of the CMC solution to 70 °C, an appropriate amount of KPS (0.18 g) was added to produce CMC free radicals. A suspension of 70% neutralized AA by 8 M NaOH, IA, MBA, and Cloisite 30B was added to the CMC solution, which was sonicated for 15 min. After 30 min, the nanocomposite hydrogel product was obtained and kept for 2 h in an oil bath to complete the polymerization reaction at 70 °C. The

Table 1 The initial feed composition of synthesized adsorbents

Hydrogel samples	Molar ratio of AA/IA (mol/mol)	KPS (g)	MBA (g)	Cloisite 30B (wt%)
Hyd (1)	0.092	0.18	0.03	0
Hyd/Cloisite 30B (2)	0.092	0.18	0.03	2
Hyd/Cloisite 30B (3)	0.092	0.18	0.03	4
Hyd/Cloisite 30B (4)	0.092	0.18	0.03	6
Hyd/Cloisite 30B (5)	0.092	0.18	0.03	8
Hyd/Cloisite 30B (6)	0.092	0.18	0.03	10
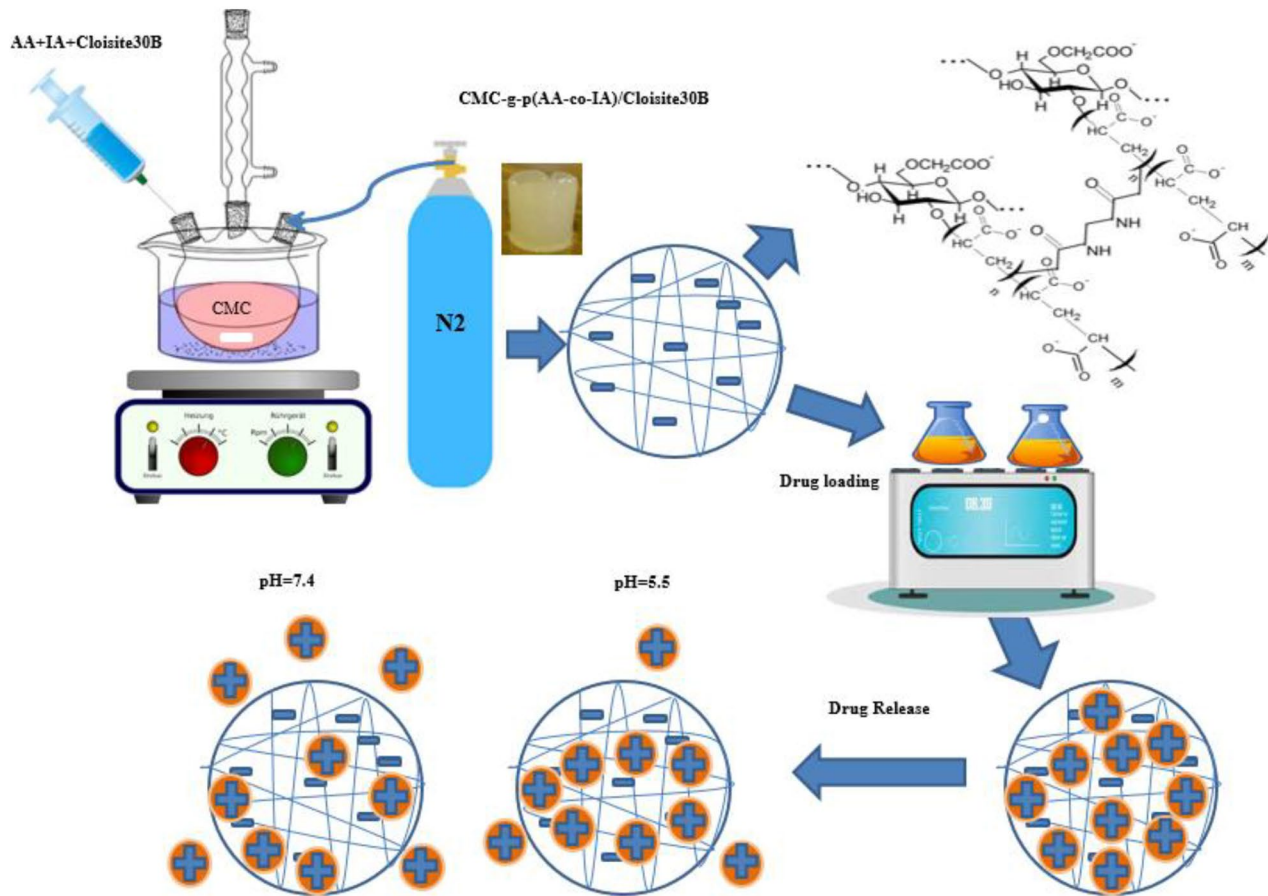
Fig. 1 A simple scheme of Hyd/Cloisite 30B preparation and drug load and release

nanocomposite hydrogel was removed from the flask and cut into small pieces with scissors. The impurities were removed by washing nanocomposite hydrogel pieces in fresh distilled water several times. Nanocomposite hydrogel pieces were dried in an oven at 60 °C for 24 h. After grounded into powder, they were sifted through 40–80 sieves for further experiments. The feed ratio and amounts of components are described in Table 1.

Swelling measurement
A determined amount of powdered hydrogel samples (0.03 g) was immersed into a buffer solution (pH 5.5 and 7.4) for 24 h to reach equilibrium swelling. The swollen

hydrogel samples were separated from the buffer solution, and the excess water was removed using tissue paper. After measuring their weight, the swelling factor (SF) is obtained using the following equation:

$$SF = \frac{W_{e,s} - W_d}{W_d} \quad (1)$$

Where $W_{e,s}$ (g), and W_d (g) are the weight of the swelled hydrogel at the equilibrium state and the weight of the dry hydrogel, respectively. Three replicates were performed on all experiments to ensure accuracy, and the mean values and error bars were reported.

Sunitinib malate loading/release

A method of soaking or equilibrating has been applied to the loading of Sunitinib malate. Dried powder samples were placed in 10 mL of 100 mg/L of Sunitinib malate solution and left in the solution until Sunitinib malate solution was sucked up. Then, the completely swollen and drug-loaded hydrogels were dried overnight in an oven at 40 °C. Equation 2 was used to compute encapsulation efficiency (EE, %).

$$EE(\%) = \frac{x}{y} \times 100 \qquad (2)$$

Where x and y denote the mass of the drug in the carrier and the initial mass of the drug, respectively, to study drug release, the dried drug-loaded nanocomposite hydrogel was immersed into a 30 mL buffer solution with different pH (5.5 and 7.4). It was shaken in a shaker incubator at 37 °C. At the desired time, 2 mL of aliquot solution was withdrawn and assayed by a UV-visible spectrophotometer at $\lambda_{max}=430$ nm to determine the concentration of the released drug. 2 mL of fresh buffer was added to the container to keep the sink condition. To plot the release profile, cumulative release (CR, %) was computed at determined time intervals (Eq. 3).

$$CR(\%) = \frac{C_i V_i + \sum\limits_{i=1}^{n} C_{i-1} V_s}{m_t} \times 100 \qquad (3)$$

Where C_i and C_{i-1} denote the concentration of released Sunitinib malate at time intervals of t and t-1, respectively, V_i is the total volume of the release medium, V_s is the withdrawn volume from the release medium, and m_t is the total initial weight of loaded Sunitinib malate. All experiments were repeated thrice. The simple scheme of Hyd/Cloisite 30B preparation, drug loading and releasing are depicted in Fig. 1.

Characterization

Fourier Transform Infrared Spectroscopy (FTIR) (Tensor 27, Bruker, Germany) was applied to identify the chemical structure of Hyd, Hyd/Cloisite 30B, and drug@Hyd/Cloisite 30B structure in the wavenumbers of 4000 to 400 cm^{-1}. The crystallinity and stability of Hyd/Cloisite 30B before and after drug loading were investigated by a X-ray diffractometer (XRD: Krisallofex D500, Siemens, Germany) equipped with CuKα irradiation ($\lambda=1.5406$ A°) operating at 40 kV and 25 mA over the scanned range of 10–70°. The morphology of Hyd, and Hyd/Cloisite 30B was assessed using scanning electron microscopy (SEM) with an accelerating voltage of 15 kV (SEM-TESCAN MIRA3-FEG). The surface of the samples was coated with a thin layer of gold after fracturing

in liquid N$_2$. The morphology of Hyd/Cloisite 30B was described using transmission electron microscopy (TEM: Philips EM 208 S operating at 100 kV).

Antibacterial activity

To assess the antibacterial effects of the samples, the well diffusion technique was employed using two types of bacteria, namely *S. Aureus* and *E. Coli.* In this method, the nutrient agar culture media were treated with 0.5 McFarland turbidity standards of bacterial activity and poured onto plates measuring 10 cm in diameter. Afterward, 0.05 g drug-loaded samples (0–10 wt%) was put in the created well on the nutrient agar culture media. After preparing the plates, they were incubated at 37 °C for 24 h. The antibacterial activity of the samples was then assessed by measuring the formation of a transparent zone surrounding the well.

MMT assay

MCF-7 human breast cancer cells and L929 cells (normal human fibroblastic cells) were used. The cell lines were cultured in DMEM supplemented with 10% FBS and 1% Penicillin-Streptomycin (100 U/ml) under standard conditions. Subsequently, the cells were seeded in a 96-well plate and incubated at 37 °C for 24 h. Once the incubation period was completed, the cells were treated with the drug-loaded Hyd/Cloisite 30B. Then, 200 µL of a solution containing 3-(4,5-dimethylthiazol-2-yl)-2,5-diphenyl tetrazolium bromide (MTT) in a 5 mg/mL concentration was introduced into the wells. The plate was then incubated at 37 °C for 24, 48, and 72 h. To dissolve the formazan crystals produced by the viable cells, 200 µL of DMSO was added to each well. The absorbance at a wavelength of 570 nm was subsequently measured using a microplate reader (Elx808, BioTek, USA) [26]. The cell viability percentage, which represents the ratio of the treated cells to the untreated controls, was calculated using Eq. 4.

$$Cell\ viability(\%) = \frac{Absorbance\ of\ treated\ cells\ at\ 570\ nm}{Absorbance\ of\ untreated\ cells\ at\ 570\ nm} \times 100 \qquad (4)$$

Results and discussion
FTIR analysis

FTIR analysis was considered to investigate the chemical structure of Hyd, Hyd/Cloisite 30B, and drug@Hyd/Cloisite 30B, and the results are demonstrated in Fig. 2. The stretching vibrations of –OH and –NH bonds overlapped at 3423 cm^{-1}. The stretching vibrations of –C=O and –C–O bonds of carboxyl groups were detected at 1732 and 1168 cm^{-1}, respectively. In the FTR spectra of Hyd/Cloisite 30B, two new peaks were seen at 528 and 455 cm^{-1}, which correspond to –Al–O and –Si–O,
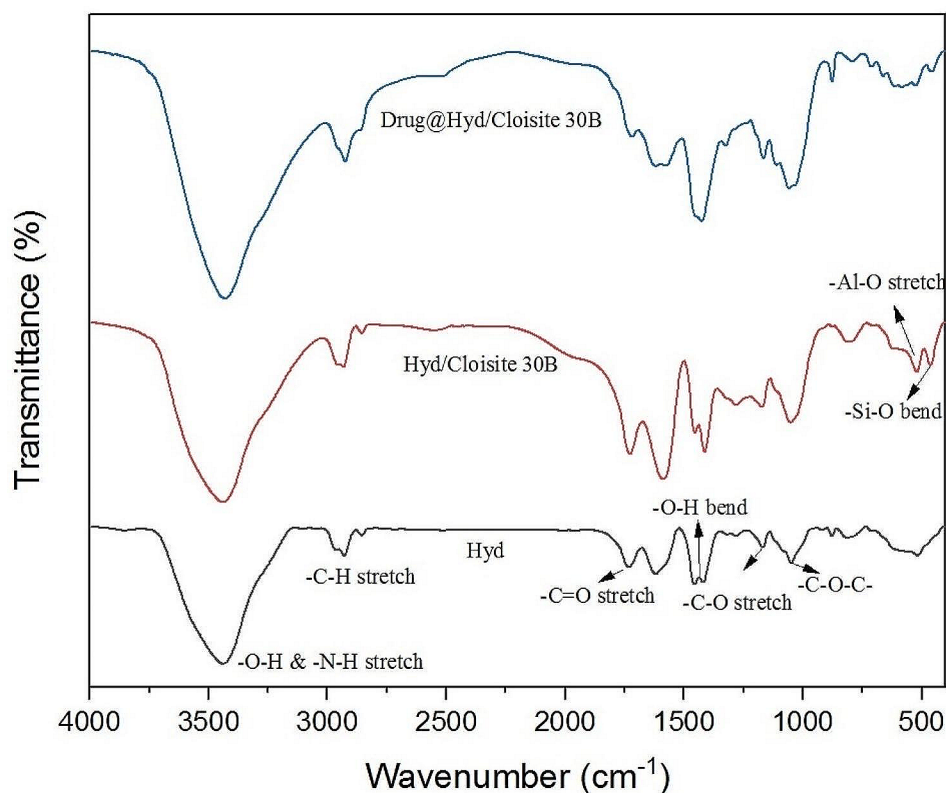
**Fig. 2** FTIR spectra of Hyd, Hyd/Cloisite 30B and Drug@Hyd/Cloisite 30B
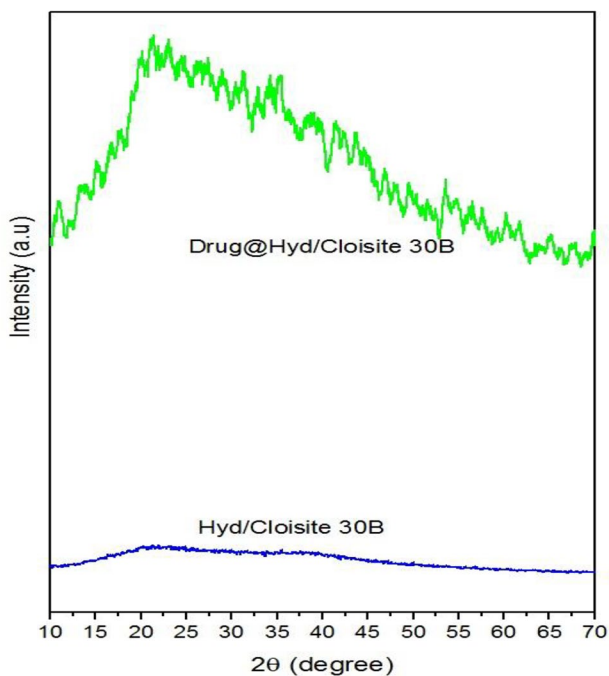
Fig. 3 XRD analysis of Hyd/Cloisite 30B before after Sunitinib malate loading

respectively. These peaks confirmed the presence of Cloisite 30B in the nanocomposite hydrogel structure [27]. FTIR analysis was performed after drug loading to verify the successful loading of Sunitinib malate on Hyd/Cloisite 30B. The intensity of overlapped stretching vibrations of −OH and −NH bonds placed at 3423 cm^{-1} was increased after drug loading, which can be related to hydrogen bond formation between the −NH group of Sunitinib malate and −OH and −NH groups of Hyd/ Cloisite 30B. Also, the intensity and position of −C=O and −C−O bands were changed after drug loading due to electrostatic interaction between the carboxyl group of Hyd/Cloisite 30B and the protonated amine group of Sunitinib malate.

XRD analysis

The results of XRD analysis of Hyd/Cloisite 30B and Hyd/Cloisite 30B after Sunitinib malate loading were demonstrated in Fig. 3. A wide broad peak exists around 2θ of 22° in the XRD pattern of Hyd/Cloisite 30B showing the amorphous structure of nanocomposite hydrogel. After drug loading, some sharp peaks were observed in the XRD pattern of drug@Hyd/Cloisite 30B, showing successful loading of Sunitinib malate.
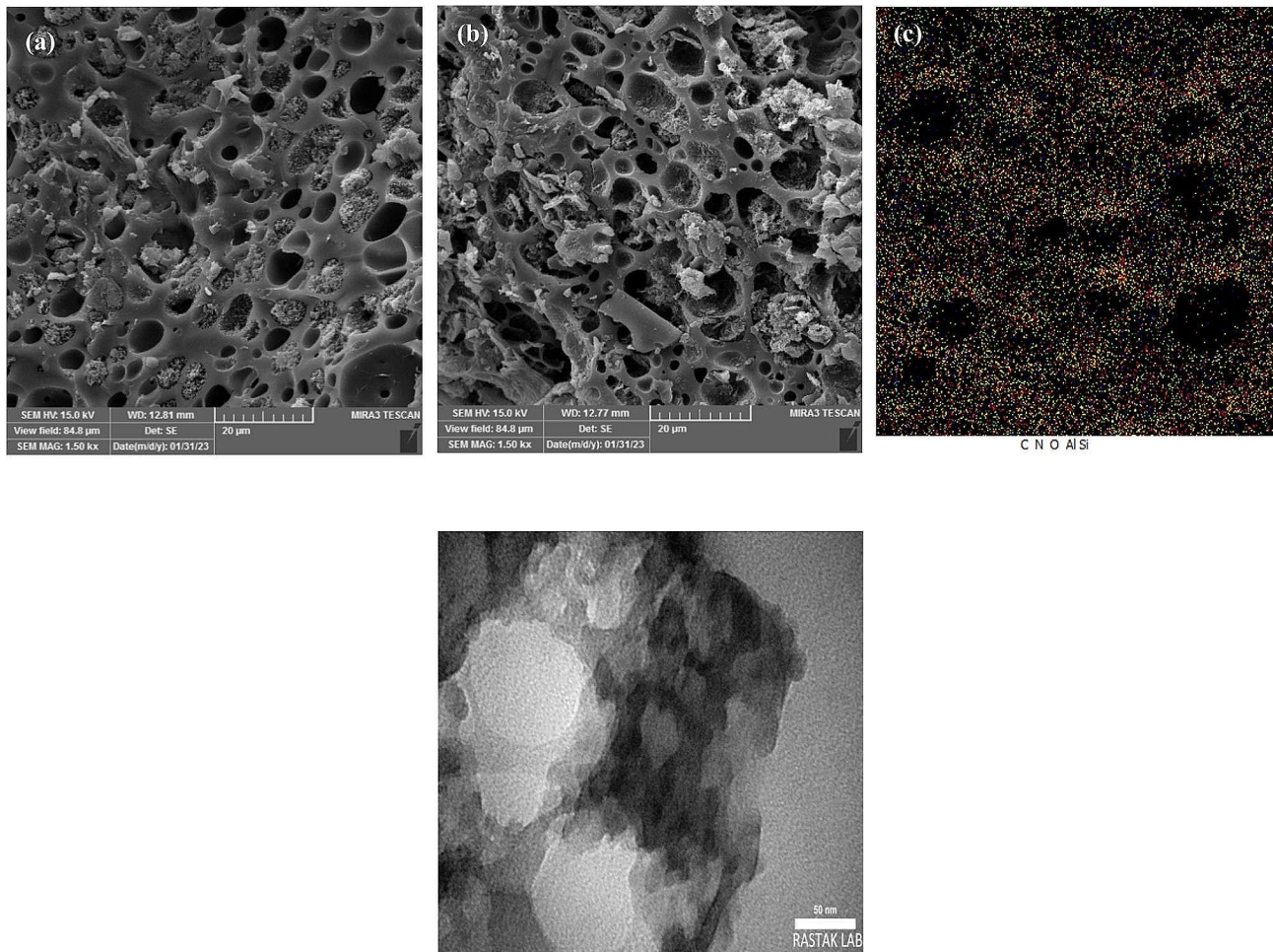
Fig. 4 SEM images of (**a**) Hyd, (**b**) Hyd/Cloisite 30B (6 wt%), and (**c**) dot mapping of Hyd/Cloisite 30B (6 wt%), and (**d**) TEM image of Hyd/Cloisite 30B (6 wt%)

Table 2 Impact of pH on swelling of samples

| Sample	Dry weight (W_d)	pH = 5.5		pH = 7.4	
		Swelled weight (W_s) ± SD	Swelling factor (SF)	Swelled weight (W_s)	Swelling factor (SF)
Hyd (0 wt%)	0.03	0.3403 ± 0.015	10.345	0.8063 ± 0.019	25.876
Hyd/Cloisite 30B (2 wt%)	0.03	0.4832 ± 0.021	15.108	0.9176 ± 0.015	29.587
Hyd/Cloisite 30B (4 wt%)	0.03	0.5418 ± 0.025	17.059	1.1897 ± 0.021	38.658
Hyd/Cloisite 30B (6 wt%)	0.03	0.7343 ± 0.019	23.476	1.2453 ± 0.010	40.509
Hyd/Cloisite 30B (8 wt%)	0.03	0.6437 ± 0.021	20.456	1.1096 ± 0.015	35.987
Hyd/Cloisite 30B (10 wt%)	0.03	0.5925 ± 0.020	18.765	1.0441 ± 0.025	33.803

SEM-dot mapping and TEM analysis

The morphology of Hyd and Hyd/Cloisite 30B (6 wt%) was investigated using SEM-dot mapping analyses. As depicted in Fig. 4a, b, a porous structure with different cavity sizes is visible in Hyd and Hyd/Cloisite 30B (6 wt%), which is suitable for carrying and releasing drugs by providing various pathways to drug diffusion. The presence of Al and Si elements, which were demonstrated by blue and green dots, respectively, proves the successful integration of Cloisite 30B nanosheets and their uniform dispersion over nanocomposite hydrogel (see Fig. 4c).

Figure 4d demonstrates the TEM image of Hyd/Cloisite 30B. The Cloisite 30B sheets were successfully exfoliated between the polymeric chains, confirming the successful formation of nanocomposite hydrogel. Also, the TEM image of Hyd/Cloisite 30B (6 wt%) displays a high distribution of Cloisite 30B nanosheets without agglomeration in the hydrogel matrix.

Swelling study

The swelling of Hyd/Cloisite 30B samples at pHs of 5.5 and 7.4 was tested, and the results are reported in
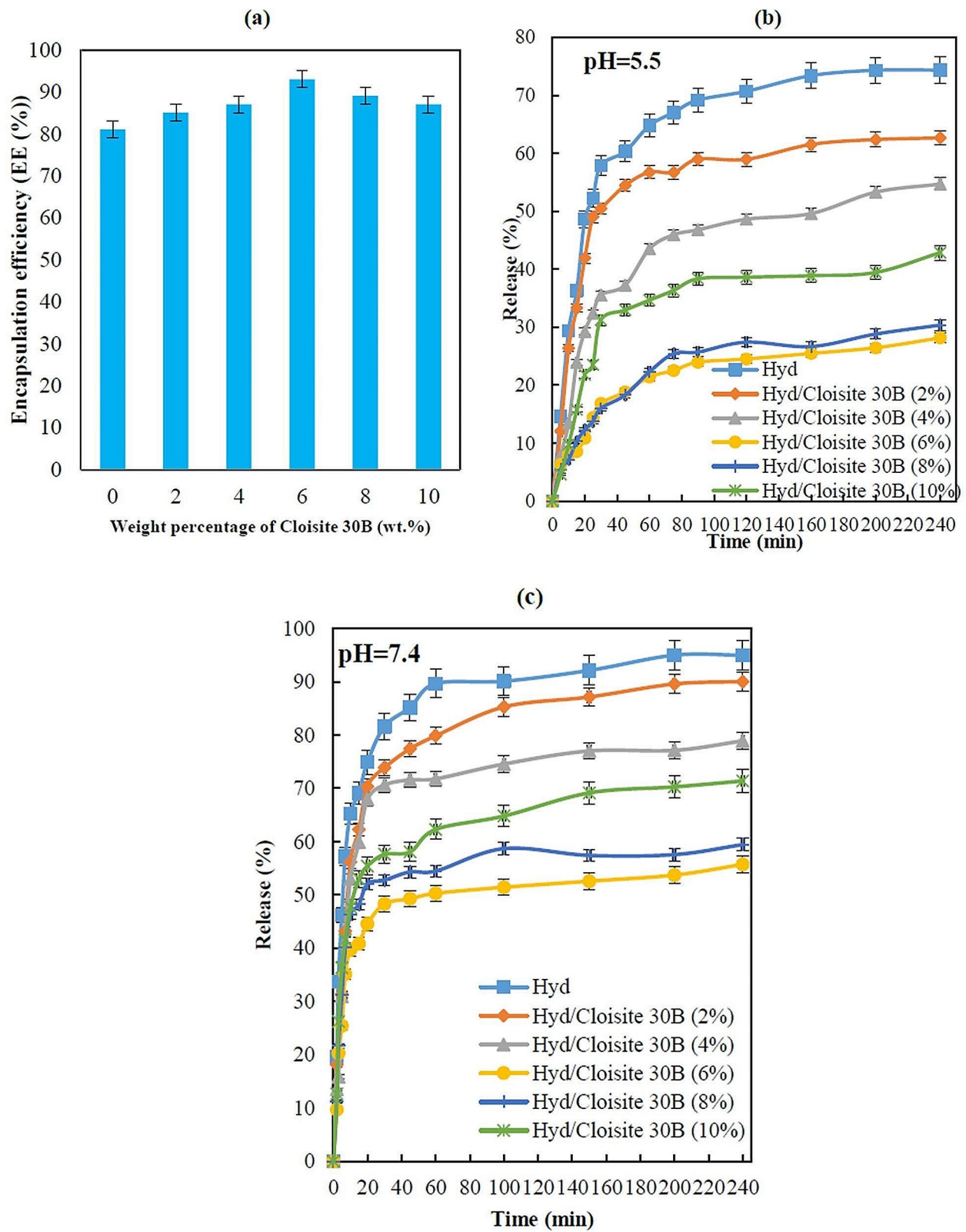
Fig. 5 The impact of Cloisite 30B content on (**a**) Encapsulation efficiency (EE (%)), (**b**) Sunitinib malate cumulative release at pH 5.5, and (**c**) sunitinib malate cumulative release at pH 7.4

Table 2. All samples showed good swelling, but the maximum swelling values were obtained at pH 7.4. When pH increases, the density of ionized carboxyl groups in the hydrogel structure is elevated. The electrostatic repulsive force between the ionized carboxyl groups causes the expansion of the hydrogel network and facilitates the diffusion of water molecules. In addition, nanocomposite hydrogel containing 6 wt% Cloisite 30B demonstrated the highest amount of swelling. By incrementing the weight% of Cloisite 30B, the content of hydroxyl groups in the structure of nanocomposite hydrogel increases, leading to more water adsorption. By further increasing the Cloisite 30B weight% from 6 wt%, swelling is reduced, which is related to the act of Cloisite 30B nanosheets as crosslinkers limiting the expansion of polymer chains. The Hyd/Cloisite 30B stability was tested and remained stable for one month at all tested pHs while the porous structure and swelling abilities of the CMC hydrogels were preserved. The stability of the hydrogel was improved by adding Cloisite 30B due to the suitable crosslinking, and no weight loss was observed.

In vitro Sunitinib malate loading/release studies

The effect of the weight% of Cloisite 30B nano-sheets on encapsulation efficiency (EE %) and release of Sunitinib malate as a function of time for 240 min was depicted in Fig. 5 (a-c). From Fig. 5a, the weight% of Cloisite 30B elevated from 0 to 6 wt%, EE value enhances from 81 to 93%. Enhancing EE by incrementing Cloisite 30B weight% can be related to more entrapping of drug molecules through hydrogen binding between the –OH group of Cloisite 30B and –N–H group of Sunitinib malate. The in vitro Sunitinib malate release by Hyd/Cloisite 30B samples was tested at pHs of 5.5 and 7.4 for 240 min. Sunitinib malate release was decreased by the increment of Cloisite 30B from 0 to 6 wt%, which lengthened the migration path needed for Sunitinib malate release. The results show that Sunitinib malate cumulative release (CR %)

from carriers is also affected by pH. Sunitinib malate CR % at pH 7.4 was higher than pH 5.5 for all samples. In Hyd's structure, abundant carboxyl groups are related to the presence of AA and IA monomers. IA has two pendant carboxyl groups with two different p_{Ka}. The p_{Ka} of the conjugated carboxyl group to methylene is 5.75, and another is 3.85. AA has a carboxyl group with p_{Ka} of 4.26. At pH 7.4, the number of dissociated carboxyl groups was increased. More electrostatic repulsion between anionic functional groups leads to the expansion of the hydrogel matrix, so the size of pores is increased, and the drug can easily diffuse to media.

The kinetic study of drug release was performed to understand the mechanism of drug release. Two kinetic models, Korsmeyer-Peppas (Eq. (5)) and Higuchi (Eq. (6)), were considered to study the release mechanism of Sunitinib malate from synthesized carriers at pH 5.5 and 7.4.

$$CR = K_{KP}t^n \tag{5}$$

$$CR = K_H t^{0.5} \tag{6}$$

Where K_{KP} and K_H donate, the rate constants of the Korsmeyer-Peppas and Higuchi models, respectively, and n represents the diffusion constant showing the mechanism of drug release. In the Korsmeyer-Peppas model, the Fickian diffusion phenomenon prevails when n is lower than 0.45 ($n \leq 0.45$). A value of n between 0.45 and 0.89 is associated with anomalous transport. The n value of ≥ 0.89 shows the predomination of the case-II transport mechanism. The values of n and K_{KP} were computed from the slope and intercept of the Ln(CR) vs. Ln(t) plot, respectively. The value of K_H was calculated from the slope of CR vs. $t^{0.5}$ plot [13].

Table 3 represents the findings of the Higuchi and Korsmeyer-Peppas model fitting. The Higuchi model shows drug diffusion. Also, Drug release from hydrogel

Table 3 The calculated kinetic parameters of Sunitinib malate release according to Higuchi and Korsmeyer-Peppas models [28]

|		Higuchi model		Korsmeyer-Peppas model		
		K_H	R^2	N	K_{KP}	R^2
Hyd (0 wt%)	pH=5.5	9.78	0.96	0.89	1.44	0.99
	pH=7.4	20.26	0.95	0.75	16.97	0.98
Hyd/Cloisite 30B (2 wt%)	pH=5.5	8.76	0.97	0.68	2.06	0.99
	pH=7.4	15.65	0.96	0.53	14.24	0.98
Hyd/Cloisite 30B (4 wt%)	pH=5.5	7.23	0.97	0.51	2.39	0.99
	pH=7.4	15.01	0.94	0.48	13.94	0.99
Hyd/Cloisite 30B (6 wt%)	pH=5.5	2.69	0.97	0.38	6.97	0.99
	pH=7.4	12.011	0.95	0.28	8.80	0.99
Hyd/Cloisite 30B (8 wt%)	pH=5.5	4.73	0.96	0.41	2.96	0.99
	pH=7.4	14.53	0.95	0.36	12.55	0.98
Hyd/Cloisite 30B (10 wt%)	pH=5.5	2.73	0.93	0.39	5.81	0.99
	pH=7.4	13.93	0.97	0.31	11.84	0.98

Sayyar *et al. BMC Biotechnology*   (2024) 24:70

Page 9 of 12
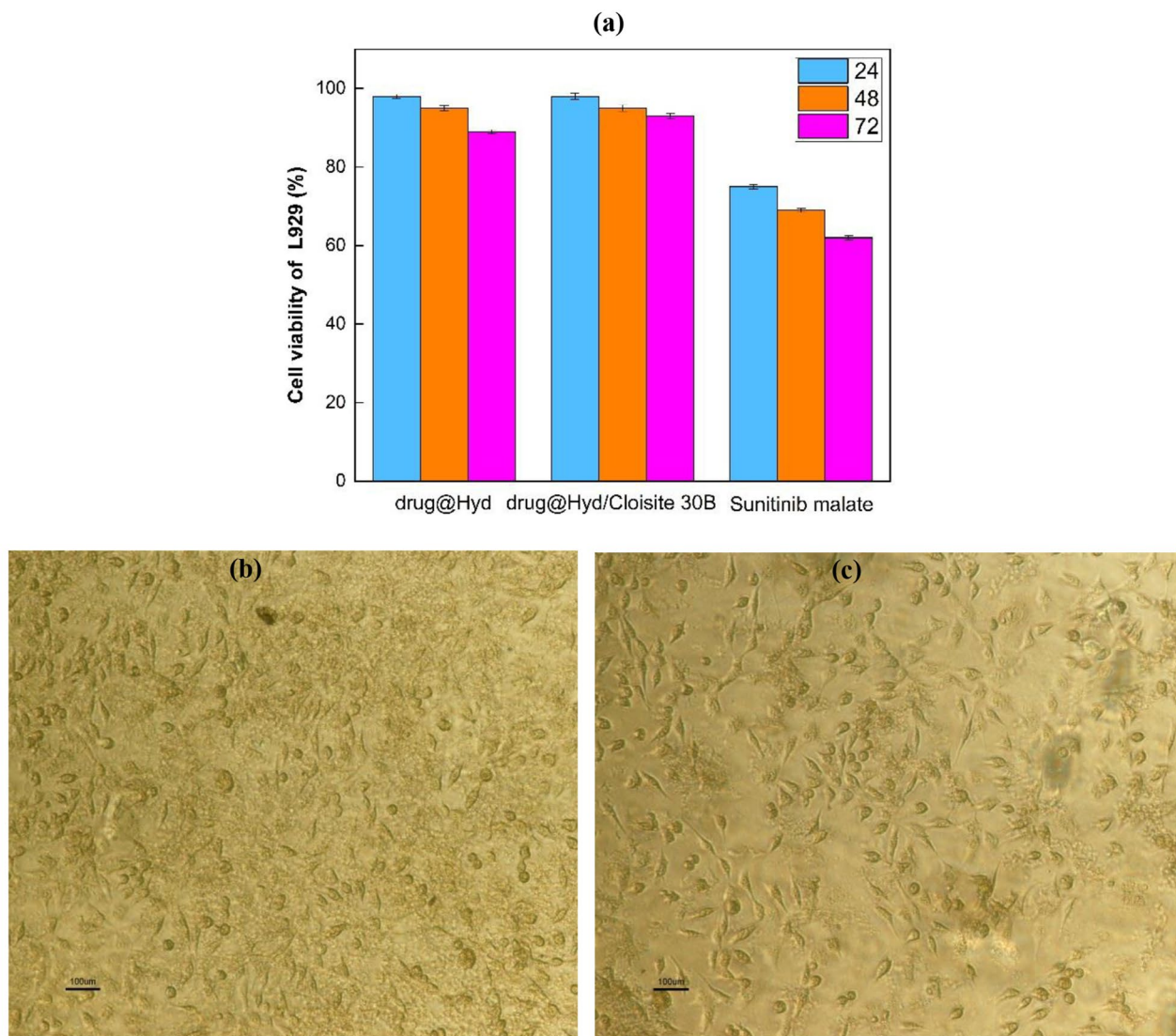
Fig. 6 (**a**) The percentage cell viability of the normal human fibroblastic cells (L929) cell lines for 24, 48 and 72 h incubation with drug@Hyd, drug@Hyd/Cloisite 30B, and pure Sunitinib malate and Cell viability of MCF-7 human breast cancer cell in (**b**) the beginning of the experiment (**c**) after treating with drug@Hyd/Cloisite 30B for 72 h

was investigated using the Korsmeyer-Peppas model because it follows various kinetic modes, including diffusion, Fickian transport, and non-Fickian transport [28]. In this study, it could be stated that the R^2 values of the Korsmeyer-Peppas model were slightly higher than those of the Higuchi model, which implied that the Korsmeyer-Peppas model was the most accurate mathematical model for investigation. The correlation coefficients (R^2) for the Korsmeyer-Peppas model were consistently above 0.98, indicating a strong linear relationship. Notably, the Korsmeyer-Peppas model is the best model to fit the release data of the carriers at pH=5.5, as evidenced by the higher R^2 values, approximately 0.99. The n values for the Sunitinib malate release from the Hyd/Cloisite 30B

were less than 0.45 at pH=5.5, indicating the release of Sunitinib malate from the carriers through Fickian diffusion [29]. Furthermore, it was observed that the R^2 values for Sunitinib malate were higher in the Korsmeyer-Peppas model compared to the Higuchi model. This indicates that the release of Sunitinib malate from the carriers followed the Korsmeyer-Peppas model, suggesting that diffusion played an essential role in the release process [30].

In vitro cytotoxicity analysis
To assess the biocompatibility, the cell viability percentage of L929 cells as normal human fibroblastic cells after being incubated with drug@Hyd, drug@Hyd/Cloisite 30B, and Sunitinib malate was measured. As shown in
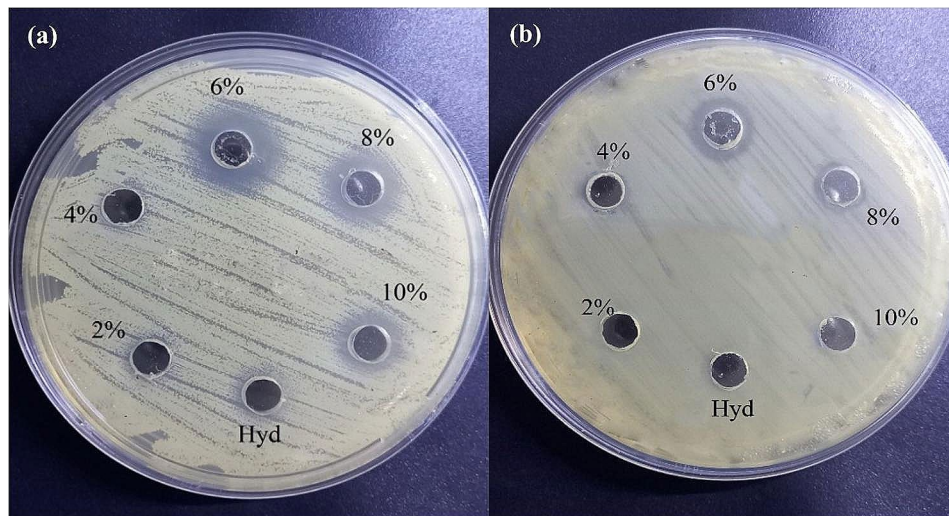
Fig. 7 Antibacterial activity of prepared samples against (**a**) S. aureus and (**b**) E. coli

Table 4 Antibacterial activity of Sunitinib malate loaded carriers against *S. Aureus* (Gram-positive) and *E. Coli* (Gram-negative)

No.	Sample	Escherichia Coli (mm) ± SD	Staphylococcus Aureus (mm) ± SD
1	drug@Hyd (0 wt%)	0	6 ± 0.45
2	drug@Hyd/Cloisite 30B (2 wt%)	0	6 ± 0.36
3	drug@Hyd/Cloisite 30B (4 wt%)	6 ± 0.12	8 ± 0.88
4	drug@Hyd/Cloisite 30B (6 wt%)	9 ± 0.45	14 ± 0.32
5	drug@Hyd/Cloisite 30B (8 wt%)	7 ± 0.98	11 ± 0.15
6	drug@Hyd/Cloisite 30B (10 wt%)	0	9 ± 0.77

Fig. 6a, the cell viability percentage of L929 cells of drug@Hyd, drug@Hyd/Cloisite 30B, and pure Sunitinib malate after 72 h was 89, 93, and 62%, respectively. The outcomes exhibited the biocompatibility of drug@Hyd/Cloisite 30B, which is higher than drug@Hyd and pure Sunitinib malate. Hyd/Cloisite 30B did not permit the Sunitinib malate to be released rapidly, leading to a decrease in the Sunitinib malate release rate and cytotoxicity. Due to its biocompatible nature and a nontoxic and biodegradable structure that enhanced biocompatibility, these carriers showed no signs of toxicity towards L929 cells. The cytotoxicity of drug@Hyd/Cloisite 30B (6 wt%) was tested by MMT assay against MCF-7 human breast cancer cells. Figure 6b and c show MCF-7 human breast cancer cells treated with Sunitinib malate loaded Hyd/Cloisite 30B (6 wt%) in the beginning of the experiment and after 72 h, respectively. After 72 h incubation, 23.82 ± 1.23% of cells survived, showing the anticancer activity of this carrier. The findings showed that the cell viability of MCF-7 cells was decreased with exposure to Sunitinib malate-loaded Hyd/Cloisite 30B nanocomposite hydrogel. Moreover, Sunitinib malate-loaded Hyd/Cloisite 30B exhibited the most pronounced inhibitory effect on MCF-7 cancer cell lines. Our results suggest that Hyd/Cloisite 30B in comparison to Hyd could potentially be applied as an efficient and safe carrier for Sunitinib malate in cancer therapy in

the way that the small parts of healthy cells were damaged. Still, most parts of cancerous cells were destroyed.

Antibacterial activity

The antibacterial activity (clear zone) of prepared samples against *E. Coli* and *S. Aureus* was assessed, and the results were represented in Fig. 7a, b, and Table 4. The prepared samples loaded with Sunitinib malate showed better antibacterial activity against *S. Aureus* bacteria than *E. Coli*. Moreover, Sunitinib malate loaded nanocomposite hydrogel sample containing 6 wt% Cloisite 30B nanosheets had the highest antibacterial activity than the other tested conditions, showing efficient drug loading and release (Fig. 7). So, drug@Hyd/Cloisite 30B (6 wt%) could be applied to treat diseases brought on by both bacteria. These results are in line with swelling and Sunitinib malate release findings.

Conclusion

This work aimed to fabricate a Cloisite 30B-incorporated carboxymethyl cellulose graft copolymer of acrylic acid and itaconic acid hydrogel (Hyd) via a free radical polymerization method for controlled release of Sunitinib malate anticancer drug. The synthesized samples were characterized by FTIR, XRD, TEM, and SEM-dot mapping analyses. The encapsulation efficiency of Hyd

and Hyd/Cloisite 30B (6 wt%) was 81 and 93%, respectively, showing the effectiveness of Cloisite 30B in drug loading. In vitro, drug release study showed that drug release from all samples in a buffer solution with pH 7.4 was higher than in a buffer solution with pH 5.5, and the cumulative drug release from Hyd/Cloisite 30B is lower than Hyd. Drug-loaded samples demonstrated better antibacterial activity towards *S. Aureus* bacteria than *E. Coli*, and maximum antibacterial activity was obtained by Sunitinib malate loaded Hyd/Cloisite 30B (6 wt%). Moreover, the MTT assay showed the anticancer activity of Sunitinib malate loaded Hyd/Cloisite 30B against MCF-7 human breast cancer cells, suggesting its potential application as a pH-regulated carrier for delivering the Sunitinib malate.

Declarations

Ethics approval and consent to participate
This article does not contain any studies with human participants or animals performed by any of the authors.

Consent for publication
Not applicable.

Competing interests
The authors declare no competing interests.

References
1. Mohammadzadeh Pakdel P, Peighambardoust SJ. Review on recent progress in chitosan-based hydrogels for wastewater treatment application. Carbohydr Polym. 2018;201:264–79.
2. Mohammadzadeh Pakdel P, Peighambardoust SJ. A review on acrylic based hydrogels and their applications in wastewater treatment. J Environ Manage. 2018;217:123–43.
3. Rakhshaei R, et al. Graphene quantum dot cross-linked carboxymethyl cellulose nanocomposite hydrogel for pH-sensitive oral anticancer drug delivery with potential bioimaging properties. Int J Biol Macromol. 2020;150:1121–9.
4. Shin Y, et al. pH-Responsive succinoglycan-carboxymethyl cellulose hydrogels with highly improved mechanical strength for Controlled Drug Delivery systems. Polymers. 2021;13(18):3197.
5. Dave PN, Macwan PM, Kamaliya B. Synthesis and characterization of biodegradable gum ghatti-cl-poly(AA-co-NIPAm)/GO based hydrogel for metformin and sodium diclofenac combined drug delivery system. Colloids Surf a. 2023;673:131815.
6. Gupta VK, et al. Antioxidant activity and controlled drug delivery potential of tragacanth gum-cl- poly (lactic acid-co-itaconic acid) hydrogel. Int J Biol Macromol. 2018;107:2534–43.
7. Parameswaranpillai J, Rangappa SM, Siengchin S. Bio-Based Epoxy Polymers, Blends, and Composites.
8. Sulatha MS, Natarajan U. Origin of the difference in structural behavior of poly (acrylic acid) and poly (methacrylic acid) in aqueous solution discerned by explicit-solvent explicit-ion MD simulations. Ind Eng Chem Res. 2011;50(21):11785–96.
9. Pomogailo AD et al. Monomeric and polymeric carboxylic acids. Macromolecular Metal Carboxylates Their Nanocomposites, 2010: p. 7–25.
10. Zhao M, et al. Itaconic acid production in microorganisms. Biotechnol Lett. 2018;40(3):455–64.
11. Zhang K, Zhang B, Yang ST. Production of citric, itaconic, fumaric, and malic acids in filamentous fungal fermentations. Bioprocessing technologies in biorefinery for sustainable production of fuels, chemicals, and polymers, 2013: pp. 375–398.
12. Gao Q, Liu J, Liu L. Relationship between morphology and itaconic acid production by aspergillus terreus. J Microbiol Biotechnol. 2014;24(2):168–76.
13. Jafari H, et al. Magnetic κ-carrageenan/chitosan/montmorillonite nanocomposite hydrogels with controlled sunitinib release. Mater Sci Engineering: C. 2021;124:112042.
14. Li C et al. Synthesis, Characterizations, and Release mechanisms of CarboxymethylChitosan-Graphene oxide-gelatin composite hydrogel for controlled delivery of drug. Inorg Chem Commun, 2023: p. 110965.
15. Akbari A, et al. Sodium alginate-halloysite nanotube gel beads as potential delivery system for sunitinib malate anticancer compound. Mater Lett. 2020;274:128038.
16. Beigmohammadi F, et al. Inhibition of Coliform Bacteria in Ultra-filtrated cheese packed in nanocomposite films containing Cloisite30B- metal nanoparticles. Nutr Food Sci Res. 2018;5:23–30.
17. Idumah CI. Novel advancements in green and sustainable polymeric nanocomposites coatings. Curr Res Green Sustainable Chem. 2021;4:100173.
18. Madusanka N, de Silva KMN, Amaratunga G. A curcumin activated carboxymethyl cellulose–montmorillonite clay nanocomposite having enhanced curcumin release in aqueous media. Carbohydr Polym. 2015;134:695–9.
19. Boruah M, et al. Biocompatible carboxymethylcellulose-g-poly (acrylic acid)/OMMT nanocomposite hydrogel for in vitro release of vitamin B 12. RSC Adv. 2014;4(83):43865–73.
20. Mohammadi R, et al. Carboxymethylcellulose/polyacrylic acid/starch-modified Fe3O4 interpenetrating magnetic nanocomposite hydrogel beads as pH-sensitive carrier for oral anticancer drug delivery system. Eur Polymer J. 2021;153:110500.
21. Sood S, et al. Controlled release of antibiotic Amoxicillin drug using carboxymethyl cellulose-cl-poly(lactic acid-co-itaconic acid) hydrogel. Int J Biol Macromol. 2017;101:612–20.
22. Yu DS. A study of an effective sunitinib–chemotherapeutic combination regimen for bladder cancer treatment using a mouse model. Urol Sci. 2014;25(2):48–53.
23. Kassem MG, Motiur Rahman AFM, Korashy HM, Brittain HG. 2012, Academic. 363–88.
24. Mokhtarpour M, Shekaari H, Shayanfar A. Design and characterization of ascorbic acid based therapeutic deep eutectic solvent as a new ion-gel for delivery of sunitinib malate. J Drug Deliv Sci Technol. 2020;56:101512.
25. Khaledian S, et al. An experimental and computational study to evaluation of chitosan/gum tragacanth coated-natural lipid-based nanocarriers for sunitinib delivery. J Mol Liq. 2021;334:116075.
26. Sayyar Z, Jafarizadeh-Malmiri H, Beheshtizadeh N. A study on the anticancer and antimicrobial activity of Curcumin nanodispersion and synthesized ZnO nanoparticles. Process Biochem. 2022;121:18–25.
27. Dimitry O, et al. Studies of particle dispersion in Elastomeric Polyurethane/Organically modified Montmorillonite Nanocomposites. Int J Green Nanotechnol. 2011;3:197–212.
28. Jain DD, Tambe SM, Amin PD. Formulation performance window for manufacturing cellulose-based sustained-release mini-matrices of highly water-soluble drug via hot-melt extrusion technology. Cellulose. 2022;29(6):3323–50.
29. Sayyar Z, Mahdavinia GR, Khataee A. Dual-drug (Curcumin/Ciprofloxacin) loading and release from chitosan-based hydrogels embedded with magnetic Montmorillonite/Hyaluronic acid for enhancing wound healing. J Biol Eng. 2023;17(1):66.

30. Rezk AI, et al. Drug release and kinetic models of anticancer drug (BTZ) from a pH-responsive alginate polydopamine hydrogel: towards cancer chemo-therapy. Int J Biol Macromol. 2019;141:388–400.

Publisher's Note